
# Vibration analysis of a steam turbine blade

R. S. Mohan[1]; A. Sarkar[2]; A. S. Sekhar[3]

[1,2,3] Indian Institute of Technology Madras, India

## ABSTRACT

Blade failure is a common problem of a steam turbine and it's failure in-service results in safety risks, repair cost and non operational revenue losses. Thus, the reliability of these blades is very important for the successful operation of a steam turbine. Dynamic analysis of a steam turbine blade in computational environment is carried out in the present work. In order to gain physical insight into the flexural dynamics of such turbine blades with the inclusion of the rotor dynamic effect, the turbine blade was approximated as a twisted cantilever beam with an asymmetric aerofoil cross-section fixed on a rigid rotor disk. Methods to validate the computational procedures for cantilever beam were established. Similar computational procedures were leveraged for the turbine blade. Critical speeds were obtained for different excitations.

Keywords: Blade vibration, Critical speed I-INCE Classification of Subjects Number(s): 75.3, 41.1, 76.4

## 1. INTRODUCTION

Blades are important component of steam turbine and its failure is a common problem. A frequent cause of turbo machinery blade failure is excessive resonant response. The most common excitation source is the non-uniform flow field generated by inlet distortion, wakes and/or pressure disturbances from adjacent blade rows. The standard method for dealing with this problem is to avoid resonant conditions using a Campbell diagram.

An in-depth study of blade vibration problems that seriously impact development of advanced gas turbine configurations are presented in [1]. Methods to predict the amplitudes of vibration of compressor blades are explained in [2]. By comparing the measured amplitudes with the fatigue properties of blade, a parameter have been established which is used in assessing the seriousness of a vibration when considering its service life. An overview of the vibration problems which are experienced in running turbines and other high-speed machinery is presented in [3]. The in-plane (lag) and out-of-plane (flap) dynamic deflections of a flexible twisted non-uniform rotating blade subjected to externally applied arbitrary dynamic loading are determined through a mode superposition approach in [4]. The main cause of failure of LP steam turbine blade is high cycle fatigue [5]. These are naturally due to the mechanical vibrations resulting in high alternating stresses. Methods of designing turbine blades against fatigue failure are presented in [6].

In the present work, we elaborate a computational procedure for determining the Campbell diagram characteristics of an industrial steam turbine blade. Also, a methodology for predicting the forced vibration response of such structures due to synchronous loading such as self-weight in rotating condition is presented.

## 2. FORMULATION

Turbine blades have their axial dimension much greater than the cross-sectional dimensions. Further, the turbine blade is rigidly attached to a stiff rotor at the root. As such to first order, they can be approximated as cantilever beams rotating about an axis perpendicular to the beam. Two modes of vibration arise in this case: - (1) vibration in the plane of rotation (lapping), (2) Vibration out of the plane of rotation (flapping). In order to gain physical insight into the flexural dynamics of such turbine blades with the inclusion of the rotor dynamic effect, the blade geometry is simplified to that of uniform and straight cantilever beams. The equation of motion for this simple model is available in the literature. The solution of these equations is also accomplished in earlier works through semi-analytical techniques. These formulations are presented in the following sections. The formulations clearly highlight the rotor dynamic effect with reference to that of the

[1] fly2rsmohan@gmail.com
[2] asarkar@iitm.ac.in
[3] as_sekhar@iitm.ac.in

well-known case of vibration of beam in a stationary frame.

### 2.1 Rotating cantilever beam

Consider a beam attached radially to a rotating disc as shown in Figure 1. Let $m(x)$ be mass per unit length, $E$ be Young modulus, $I$ be area moment of inertia and $f(x,t)$ be the loading per unit length of the beam. Consider a differential element of length $dx$ at the axial position $x$. The forces induced on this different element are: - 1. Shear force ($V$) 2. Axial force ($T$) at the cross-section caused due to centrifugal effect. Also, the differential element experiences a bending moment ($M$) as shown in Figure 2. Axial force due to centrifugal effect is given by

$$T = \int_x^l m(x)\Omega^2(r+x)dx. \tag{1}$$

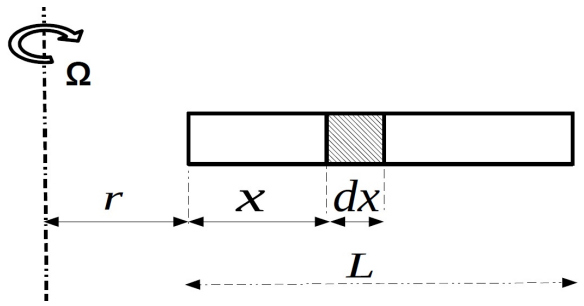


Figure 1 – Beam rotating at speed Ω

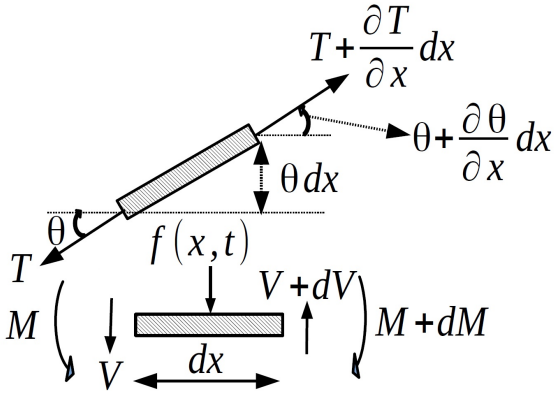


Figure 2 – Axial force acting on '$dx$'

As shown in Figure 2, the deformation of the beam enforces non-collinearity of the axial forces acting on either side of the differential beam element. This in turn leads to an additional moment acting in the opposite sense of the bending moment (refer Figure 2). Thus, the effect of rotation is to resist the deflection which in other words implies stiffening of the structure. Alternatively, if observed on a rotating frame moving at the same angular velocity as the blade, the centrifugal action creates a pre-stress (equivalently pre-strain). Thus, the rotor dynamic analysis in such cases is equivalent to the dynamic analysis of a pre-stressed structure in an inertial frame. The governing equation of a rotating Euler-Bernoulli cantilever beam is given by [7]

$$\frac{\partial^2}{\partial x^2}\left(EI_2\frac{\partial^2 W}{\partial x^2}\right) + m\frac{\partial^2 W}{\partial t^2} - \frac{\partial}{\partial x}\left(T\frac{\partial W}{\partial x}\right) = f(x,t). \tag{2}$$

In the Equation (2) the first two terms are identical with the governing equation of the Euler-Bernoulli beam [8]. The third term represents the rotor dynamic effect. A semi-analytical procedure involving Galerkin approximation was described in [7] to obtain the natural frequency. Natural frequency of rotating cantilever beam is given by

$$\omega^2 = \omega_n^2 + \Omega^2\left[\frac{1}{2}\frac{\int_\gamma^1 (1-\chi^2)\left(\frac{d\hat{W}}{d\chi}\right)^2 d\chi}{\int_\gamma^1 \hat{W}^2 d\chi}\right]. \tag{3}$$

Where, $\chi = \frac{x}{l}$, $\omega_n$ is the $n^{th}$ natural frequencies and $W$ is the corresponding mode shape of the non-rotating beam. From the equation above, it may be noted that the rotordynamic effect increases the natural frequency of the rotating beam as is expected due to the stiffening effect discussed earlier.

### 2.2 Shared eigenpair

An equivalence between a rotating and a non-rotating beam is established in [9]. It is found that a non-rotating beam with uniform flexural stiffness $EI_1$ and a rotating beam with varying flexural stiffness $EI_2(x)$ have the same $j^{th}$ eigenpair provided the following relation is satisfied

$$EI_2(x) = \frac{\int\left(\int((EI_1(x)\phi_j'')'' + (T(x)\phi_j')')dx\right)dx}{\phi_j''} \tag{4}$$

Using these results, dynamic analysis of the rotating beam is validated in the present work.

# 3. VALIDATION

## 3.1 Modal Analysis of Straight uniform Beams

Modal analysis of rotating structures through FEA is performed and validated. For inclusion of the rotor dynamic effect, a pre-stressed modal analysis is performed. This entails performing a sequential static and dynamic analysis. Through static analysis, the stresses and the displacements due to the inertial load is calculated. Rotational speed ($\Omega$) is given as inertial velocity (in $rad/s$) for all elements in static analysis. These results are then used in the modal analyses. FE model of a rotating beam having properties as listed in Table 1 is developed in ANSYS. Results are validated with the semi-analytical results obtained by solving Equation (3) and they compare well.

Table 1 – Properties of beam

| Property | Value |
|---|---|
| Length ($L$) | $0.60\ m$ |
| Elasticity modulus ($E$) | $2\times10^{11}\ Pa$ |
| Mass density ($\rho$) | $7840\ kg/m^3$ |
| Cross - Sectional area ($A$) | $2.40\times10^{-4}m^2$ |
| Moment of inertia ($I$) | $2\times10^{-9}m^4$ |

Table 2 – Comparison of natural frequencies for a rotating straight beam. $L$ and $F$ denotes lateral and flexural vibration modes, respectively.

| Mode | $\Omega$=25 $Hz$ | | | $\Omega$=50 $Hz$ | | |
|---|---|---|---|---|---|---|
| | Analytical | Ansys | | Analytical | Ansys | |
| | | Beam189 | Solid186 | | Beam189 | Solid186 |
| **1L** | 35.48 | 35.33 | 35.04 | 59.14 | 58.14 | 59.77 |
| **1F** | 60.86 | 60.77 | 60.83 | 77.08 | 76.80 | 76.86 |
| **2L** | 155.62 | 155.41 | 153.65 | 190.71 | 190.38 | 184.01 |

## 3.2 Modal Analysis of Twisted beam

Rotating cantilever beams having twist angle ($\phi$) is analysed here. FE model of a cantilever beam fixed to a rigid hub of radius ($r$) having twist angle ($\phi$) with properties as listed in [10] is generated in ANSYS. Meshing is performed using SOLID186 element due to presence of twist in the beam. Pre-stressed modal analysis is performed as discussed above. Frequencies obtained from ANSYS are non-dimensionalized by $\omega_{non} = \omega\sqrt{\frac{\rho Al}{D}}$ and are compared with [10]. Table 3 shows the comparison of results obtained for the non-dimensional natural frequencies ($\omega_{non}$) from the ANSYS simulation with that reported in [10]. The results are in good agreement.

Table 3 – Comparision of simulation results for natural frequencies of twisted beam with [10]. $L$, $F$ and $T$ denotes lateral, flexural and torsional vibration modes, respectively.

| Mode | Ref [10] | ANSYS | Ref [10] | ANSYS | Ref [10] | ANSYS | Ref [10] | ANSYS |
|---|---|---|---|---|---|---|---|---|
| | $\Omega/\omega$ = 0.5 & $\phi$ = 0 | | $\Omega/\omega$ = 1.5 & $\phi$ = 0 | | $\Omega/\omega$ = 0.5 & $\phi$ = 30 | | $\Omega/\omega$ = 1.5 & $\phi$ = 30 | |
| **1F** | 4.24 | 4.27 | 8.28 | 8.33 | 4.23 | 4.18 | 8.16 | 8.14 |
| **2F** | 21.29 | 21.01 | 22.4 | 22.69 | 19.6 | 19.18 | 24.52 | 24.05 |
| **1T** | 22.02 | 22.15 | 27.75 | 27.83 | 28.01 | 24.84 | 28.57 | 25.67 |
| **3F** | 60.54 | 60.6 | 66.54 | 62.46 | 50.47 | 55.36 | 61.42 | 60.1 |

## 3.3 Modal Analysis Validation Using Shared Eigenpair

The validation of the modal analysis of rotating straight beams is also performed using the shared eigenpair method. Towards this end, an equivalent model of a rotating beam is developed which has the same fundamental frequency and mode shape as a non-rotating uniform beam with properties as given in Table 1. The equivalent rotating beam has varying flexural stiffness which is calculated as per equation (4). Sample calculations are presented for the case of identical fundamental mode between a uniform non-rotating cantilever beam to a non-uniform rotating cantilever beam. The flexural stiffness of the later depends on the rotational speed [9]. The flexural stiffness is plotted as a function of the axial coordinates for different rotational speeds in Figure 3.

Continuous rotating beam with varying flexural stiffness along the length can be approximated to a stepped beam having multiple sections of constant flexural stiffness. To reduce the computational effort, flexural stiffness at 30 sectional points are obtained. Further, in the present implementation area moment inertia ($I$) is

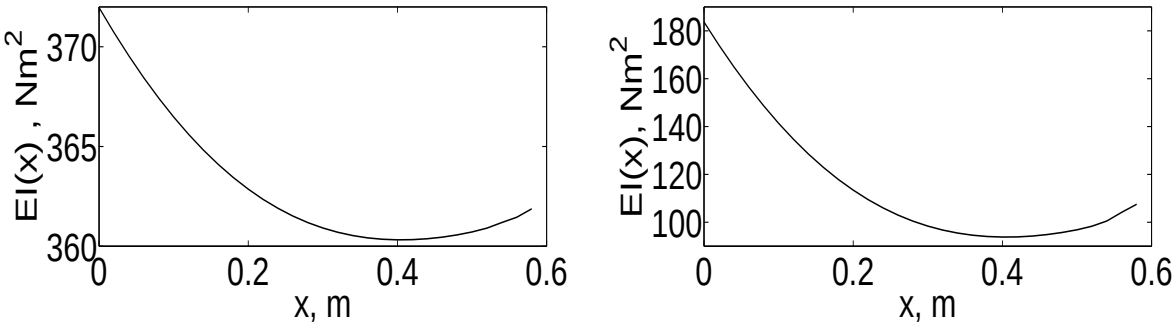


Figure 3 – Flexural stiffness function varying along the length for a beam rotating at 38 rad/s (left) and 100 rad/s (right).

considered to be constant along the beam and hence elastic modulus alone varies along the length to get the desired non-uniform flexural stiffness. FE model of a rotating beam with varying elastic modulus as described above is generated in ANSYS. The natural frequencies of the equivalent rotating beam is obtained through the simulation, whereas analytical formula is employed for determining the natural frequency of the non-rotating uniform equivalent beam. The results of natural frequencies for these beams are tabulated in Table 4. As noted from the table, the equivalence is valid only for the first flexural mode. Similar, equivalence can be constructed for the other modes also using equation (3). Also, the 1st natural frequency of a rotating beam converge to the 1st natural frequency of static nonrotating beam as the number of sections of constant elastic modulus increases.

Table 4 – Natural frequencies (in $Hz$) of a stationary beam and an equivalent rotating beam having the same first eigen pair.

| **Mode** | **Static beam** | **Rotating beam** | |
|---|---|---|---|
| | **Analytical** | **38** $rad/s$ | **100** $rad/s$ |
| **1F** | **22.66** | **22.797** | **22.752** |
| **1L** | 54.39 | 33.279 | 37.07 |
| **2F** | 142.03 | 87.719 | 87.524 |
| **2L** | 340.86 | 186.88 | 187.09 |
| **3TB** | 397.71 | 222.87 | 222.42 |

Mode shapes for both the beams are extracted from ANSYS simulation. Mode shapes also compare well as shown in Figure 4.

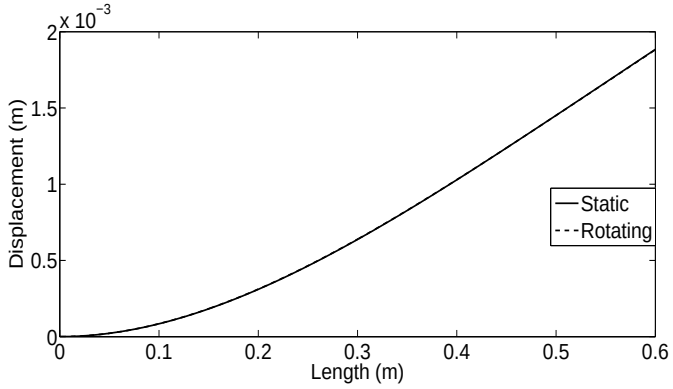


Figure 4 – Fundamental Mode Shape of a stationary beam and an equivalent rotating beam.

### 3.4 Forced vibration analysis of straight beam

FE model of a simple cantilever beam having properties listed in Table 1 is generated in ANSYS. For pre-stressed harmonic analysis, static analysis is to be performed before harmonic analysis. Rotational speed ($\Omega$ = 50 $Hz$) is given to all elements as inertial velocity in static analysis. Forcing in the form of the first

mode shape is applied in the harmonic analysis. Eigenvectors of rotating cantilever beam are orthogonal [4]. Orthogonality of mode shapes disallows other modes and their corresponding frequencies to be exhibited in the response. Figure 5 shows the response at different points over frequencies and single peak is observed at first natural frequency only($1^{st}$ Lateral frequency). The maximum response observed at the free end is 0.21 *mm*. This validates the computational procedure for harmonic analysis in ANSYS.

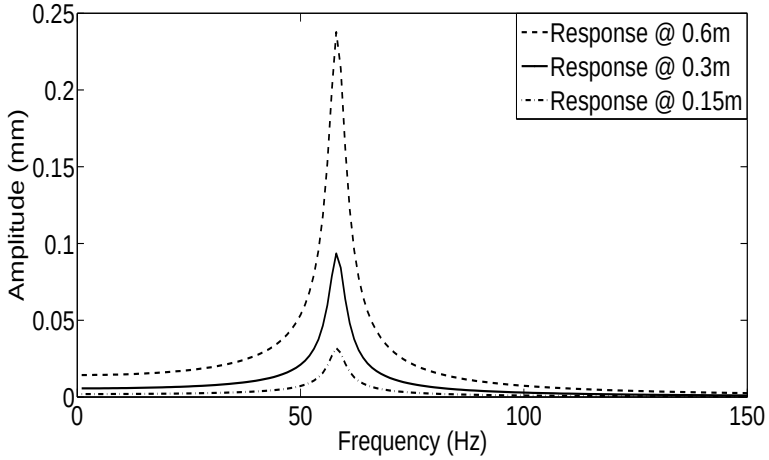


Figure 5 – Response at different point for a cantilever beam rotating at 50 Hz.

### 3.5 Forced Vibration Analysis Using Shared Eigenpair

As discussed earlier, non-rotating beam having uniform cross section will have same $j^{th}$ eigenpair as a rotating beam with varying flexural stiffness provided Equation (4) is satisfied. FE model of a rotating cantilever beam having 30 sections of elastic modulus was generated in ANSYS. First static analysis is performed in which rotational speed of 50 $Hz$ is given to all elements as inertial velocity. Forcing in the form of the first mode shape is applied in the harmonic analysis. Results are compared with non-rotating cantilever beam having uniform cross-section and forcing identical to the first mode shape. As the first eigen pair between the rotating and the non-rotating beam match, the forced response (in the form given as above) is also expected to match. Figure 6 compares the response of rotating cantilever beam having varying elastic modulus with that of non-rotating cantilever beam having constant flexural stiffness at different locations.

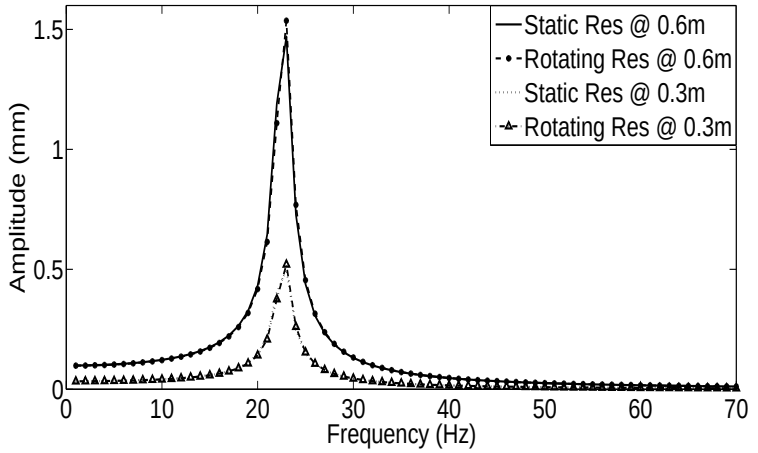


Figure 6 – Response of static and equivalent rotating beam($\Omega$ = 50 Hz) obtained from harmonic analysis.

## 4. MODAL ANALYSIS OF TURBINE BLADE

Rotating flexible structures like turbine blades are often idealized as rotating cantilever beams. The procedure followed in ANSYS to perform modal and harmonic analysis for rotating cantilever beam, respectively are discussed in the above sections. The obtained results compare well with the analytical results and hence this validates the computational procedure. The same computational procedure is leveraged for the analysis of turbine blade structure for its operational speed i.e., 0 $Hz$ to 50 $Hz$. To this end, the following steps were performed:

- Geometric 3D modeling of the turbine blade in CATIA V5 from the drawings.
- The solid model generated above is used to develop the FE model in ANSYS.
- Modal analysis is performed and Campbell diagram is plotted for operational speed i.e., 0 $Hz$ to 50 $Hz$.
- Critical speeds for synchronous and asynchronous excitation is determined from the Campbell diagram.
- Considering only self-weight in the rotating frame, harmonic analysis is performed.
- A stress analysis is performed to evaluate the reliability of the component.

### 4.1 Non-rotating turbine blade

Solid 3D model of the turbine blade was developed in CATIA V5. Figure 7 shows the modeled turbine blade. The above model was imported in ANSYS to develop FE model as shown Figure 8. Using SOLID186 element, hexahedral mesh was generated. All degrees of freedom present in the bottom surfaces are constrained as they are attached to rigid rotor disk. The FE model was used to obtain the mode shapes and natural frequencies for the turbine blade in a stationary reference frame. The natural frequencies obtained are listed in Table 5. The mode shapes observed for of stationary turbine blades are flexural(F), axial or edge bending(EB) and torsional modes(T). Figure 9 shows the first four modes of the turbine blade in stationary frame.

Figure 7 – Geometric model of turbine blade.

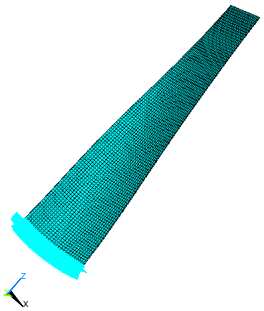

Figure 8 – FE model of turbine blade.

Table 5 – Natural frequencies for stationary turbine blade.

| Mode | Natural Frequency(Hz) | | |
|---|---|---|---|
| | 9020 Elements | 13332 Elements | 55913 Elements |
| 1F | 71.307 | 71.319 | 71.331 |
| 2F | 173.35 | 173.37 | 173.39 |
| 1T | 295.84 | 295.84 | 295.82 |
| 1EB | 398.08 | 398.11 | 398.12 |

### 4.2 Modal Analysis of Rotating Turbine Blade

A rotating turbine blade has larger bending stiffness than a stationary blade because rotation leads to stiffening effect due to the centrifugal force. The stiffening effect further depends on the rotational speed. Thus, in such structures natural frequency is a function of rotational speed and they are presented in the form of Campbell diagram.

As in the case of beams, prestressed analysis is performed by doing a static analysis before the modal analysis so that all the stresses and displacements, which are created by the centrifugal force, are included into the modal analysis. In static analysis, rotational speed (in $rad/s$) is applied to all elements as inertial velocity. All the modal analyses were done with the QR Damped method because it works best with big models and damping can be included. The same computational procedure in ANSYS is performed for different rotational speeds. The obtained natural frequencies for different rotational speeds are listed in Table 6 and Campbell diagram is plotted as shown Figure 10. Mode shapes obtained through the FEM analysis is presented in Figure 11. These mode shapes are computed for a rotational speed of $50Hz$ (maximum speed in the operating range). The mode shape contour plots are presented in the form of sum of deformations in the three orthogonal directions in Figure 11. It has been observed that the nature of these mode shapes remain largely unaffected by the rotational speed.

The following conclusions are drawn from the Campbell diagram

- Flexural natural frequency increases as the rotational speed increases. This observation is similar to that

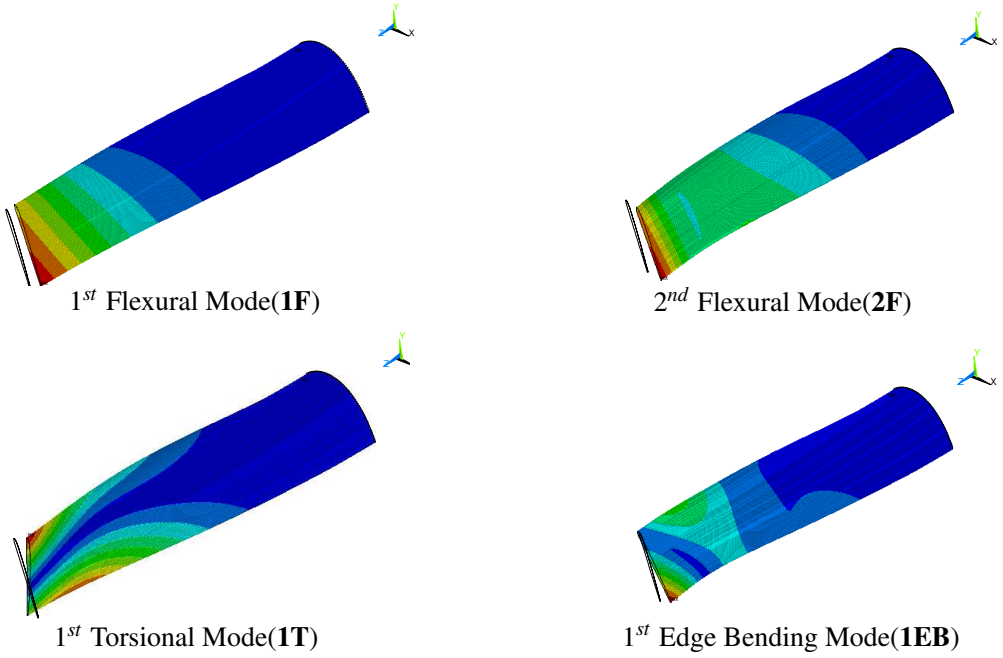


Figure 9 – Mode shapes of the turbine blade in stationary frame.

Table 6 – Natural frequencies for different rotational speeds.

| Mode | Rotational Speed (Hz) | | | | | |
|---|---|---|---|---|---|---|
| | 0 | 10 | 20 | 30 | 40 | 50 |
| 1F | 71.319 | 72.77 | 76.833 | 82.816 | 89.966 | 97.697 |
| 2F | 173.37 | 174.78 | 178.93 | 185.59 | 194.41 | 204.95 |
| 1T | 295.84 | 296.43 | 298.18 | 301.01 | 304.82 | 309.53 |
| 1EB | 398.11 | 399.38 | 403.16 | 409.32 | 417.66 | 427.89 |

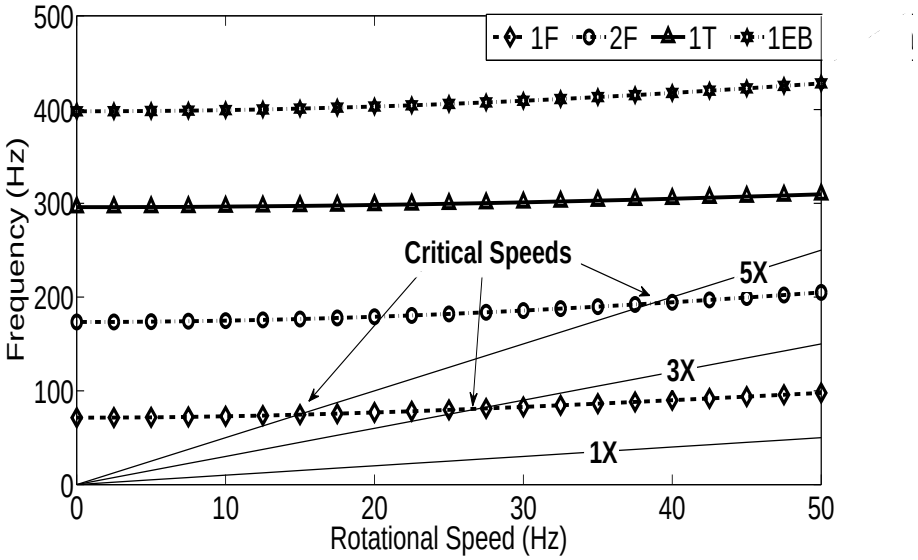


Figure 10 – Campbell diagram of the steam turbine blade.

in beams and is explained due to the centrifugal stiffening effect.

- The torsion mode frequency is almost constant over the rotational speed. This is because the torsional mode is unaffected by the centrifugal load acting in the axial direction.

- For the first harmonic no critical speed is observed in the operating speed range.
- Critical speeds occur if the excitation frequencies coincide with the natural frequency of the rotating structure. The excitation frequency itself may be synchronous to the rotational speed (1X) or multiples of it (2X, 3X, ...). These excitation frequencies are represented as straight lines in the Campbell diagram. For example, synchronous excitation (1X) is represented as a straight line with unit slope. Intersection of these lines with the natural frequency curves indicate critical speed. Using this procedure, critical speeds for different excitation frequencies are computed. These are tabulated in Table 7
- No synchronous critical speeds are observed from the results. However, higher order critical speeds exist within the operating range. These may be excited under operating conditions.

Table 7 – Critical speeds of the turbine blade for different excitation.

| Excitation | Critical Speeds (Hz) |
|---|---|
| **1X** | -No- |
| **2X** | 48.1 |
| **3X** | 26.95 |
| **4X** | 19.1 |
| **5X** | 14.9 & 38.62 |

## 5. HARMONIC ANALYSIS OF TURBINE BLADE

Harmonic vibration analysis of the turbine blade is conducted employing the same computational methodology as discussed for the case of beams and 3% of damping was assumed. The force considered in this case is the turbine self-weight. As the turbine rotates in a vertical plane, the self-weight imposes a synchronous excitation on the transverse vibration. Critical stress region is found from the stress contour obtained by performing harmonic analysis. Figure 12 and Figure 13 show the von Mises stress contours for a blade rotating at 50 $Hz$. The stress contours are plotted for the first and second natural frequencies (97 $Hz$ and 204$Hz$), respectively. The maximum stress observed at these frequencies are 9.01 $MPa$ and 10.13 $MPa$ respectively. The region of critical stress is as shown in the Figures 12 & 13. The von Mises stress variations with frequency at these critical nodes are plotted in Figure 14 and Figure 15, respectively.

As observed from these results, the stress in the material is well below the endurance limit ( 270 $MPa$). Thus, for the present loads the structure may be considered safe. It may be noted that for the present simulation the geometry of the root of the turbine blade was not incorporated. Instead, complete fixity at the root section was assumed. It is expected that the complicated geometry of the root will induce further stress concentration factors. However, as the factor of safety in the present design is quite high, this effect will not cause failure in the structure. Additionally, fluid and thermal loads present in the operating condition may result in higher stresses.

## 6. CONCLUSION

In the present work a computational procedure for vibration analysis of rotating turbine blades is developed. The procedure is rigorously validated using benchmark results available in the literature. From the mathematical model, it is appreciated that the centrifugal effect due to rotation causes pre-stressing in the structure which is equivalent to additional stiffness. It is found that this rotordynamic effect causes change in natural frequencies, critical speeds and vibration response of the structure. The present analysis is limited to the consideration of self-weight alone. Under this loading action the design is inferred to be reliable. However, major additional loads in form of fluid and thermal loads are not accounted in this analysis.These may induce additional stresses and further investigation towards this end needs to be carried out.

## REFERENCES

1. A. V. Srinivasan, "Flutter and Resonant Vibration Characteristics of Engine Blades," *Journal of Engineering for Gas Turbines and Power.*, vol. 119, no. 4, pp. 742-775, 1997.

2. E. K. Armstrong, "Recent Blade Vibration Techniques," *Journal of Engineering for Gas Turbines and Power.*, vol. 89, no. 3, pp. 437-444, 1967.

3. D. J. Ewins, "Control of vibration and resonance in aero engines and rotating machinery - An overview," *International Journal of Pressure Vessels and Piping.*, vol. 87, no. 9, pp. 504-510, 2010.

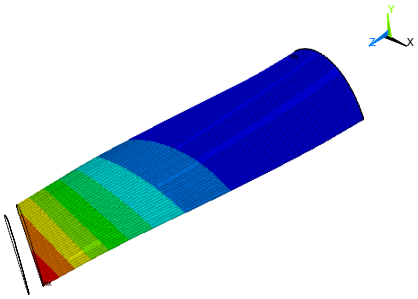

1$^{st}$ Flexural Mode(**1F**)

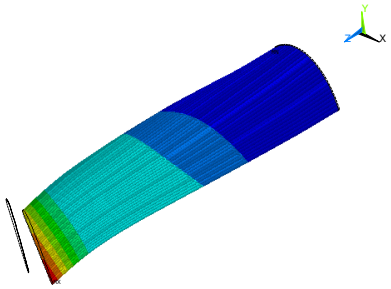

2$^{nd}$ Flexural Mode(**2F**)

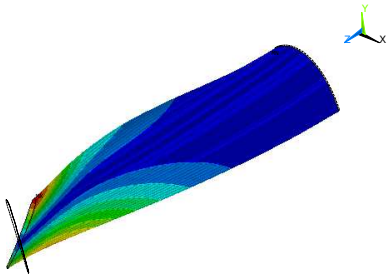

1$^{st}$ Torsional Mode(**1T**)

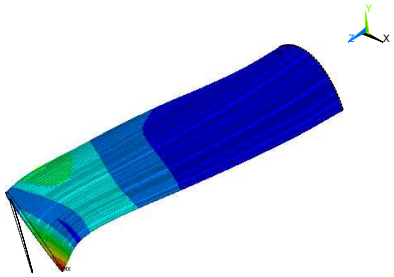

1$^{st}$ Edge Bending Mode(**1EB**)

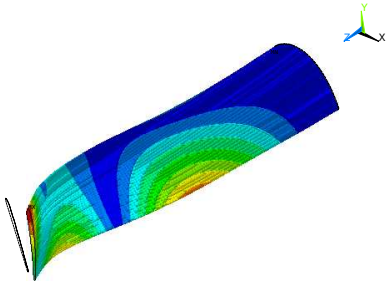

3$^{rd}$ Flexural Mode(**3F**)

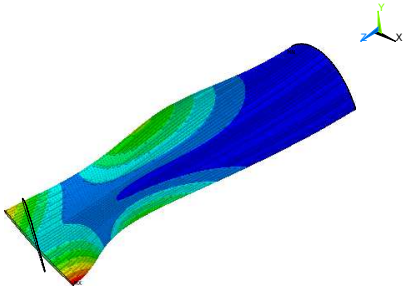

2$^{nd}$ Torsional Mode(**2T**)

Figure 11 – Mode shapes of the rotating turbine blade.

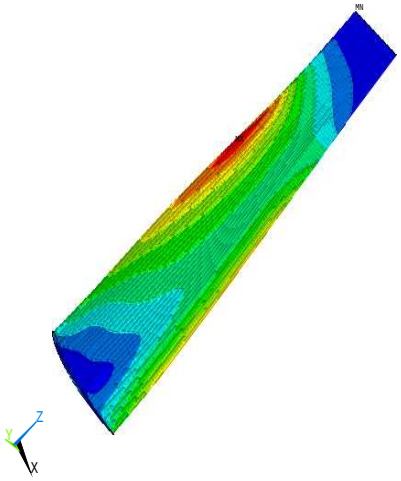

Figure 12 – Stress contour (in *MPa*) at the natural frequency corresponding to 1F mode (92 *Hz*).

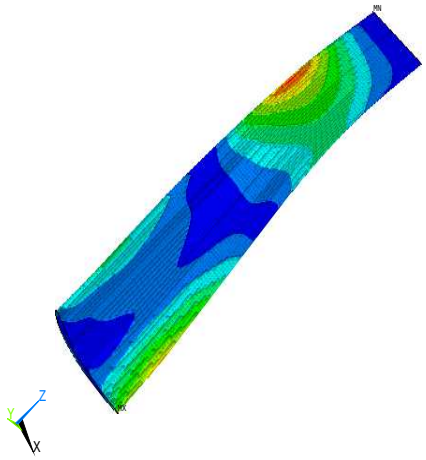

Figure 13 – Stress contour (in *MPa*) at the natural frequency corresponding to 2F mode (204 *Hz*).

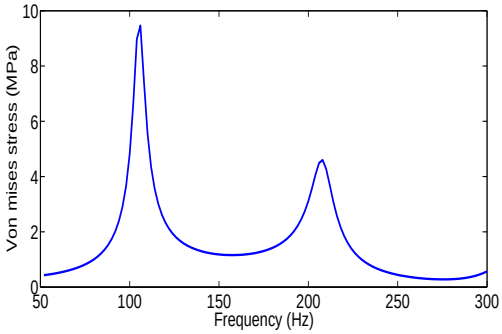


Figure 14 – Stress variation over frequency for the critical location 1 (shown in Fig 12).

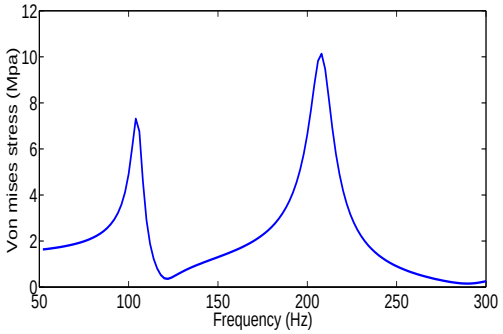


Figure 15 – Stress variation over frequency for the critical location 2 (shown in Fig 13).

4. A. G. Hernried, "Force Vibration Response of a Twisted Non-uniform Rotating Blade," *Computers & Structures.*, vol. 41, no. 2, pp. 207-212, 1991.

5. D. Ziegler, M. Puccinelli, B. Bergallo, and A. Picasso, "Investigation of turbine blade failure in a thermal power plant," *Case Studies in Engineering Failure Analysis.*, vol. 1, no. 3, pp. 192-199, 2013.

6. R. B. Heywood, *Designing Against Fatigue.*, Chapman and Hall, 1962

7. G. Genta, *Dynamics of Rotating Systems.*, Springer, 2005

8. S. S. Rao, *Machanical vibrations.*, Prentice Hall, 2011

9. A. Kumar and R. Ganguli, "Rotating Beams and Non-rotating Beams With Shared Eigenpair," *Journal of Applied Mechanics.*, vol. 76, no. 5, pp. 1-14, 2009.

10. V. Ramamurti and R. Kielb, "Natural Frequencies of Twisted Rotating Plates," *Journal of Sound and Vibration.*, vol. 97, no. 3, pp. 429-449, 1984.